Chapter III

Localised Surface Plasmon Resonance Based Sensing via Plasmonic Nanofilms

CHAPTER III
LOCALISED SURFACE PLASMON RESONANCE BASED SENSING VIA PLASMONIC NANOFILMS

- *The study emphasizes on localized surface plasmon resonance (LSPR)-based sensing systems for detecting various milk adulterants.*
- *Selectively functionalized silver nanoparticles (AgNPs) immobilized on the glass substrates were used for sensing melamine and hydrogen peroxide in milk.*
- *Significant plasmonic peak shifts were observed upon interaction with the adulterants.*
- *These shifts were quantified to determine the limit of detection (LOD) values which were found to be 10.48 ppb and 2.42 ppb, for melamine and hydrogen peroxide, respectively.*

3.1 Introduction

Plasmonic nanostructures (NSs) display outstanding optical properties that can be finely adjusted through factors such as shape, size, and composition, along with change in refractive index of their external media. These unique characteristics enable their versatile application in various domains, including sensing such as detection of heavy metals (HM), pesticides, food adulterants, various other toxic chemicals and contaminants [1,2].

In the recent era, significant attention has been directed towards utilizing plasmonic materials for sensing, particularly in detecting harmful adulterants that are deliberately introduced into food products. Among these, milk stands out as the most adulterated items worldwide. Various adulterants are added to milk for different purposes, such as extending its shelf life, falsifying its protein content, etc. Melamine, for instance, is often added to increase the apparent protein level by boosting the nitrogen content whereas hydrogen peroxide is utilised to increase the shelf life of milk. However, their consumption, can cause serious health hazards [3,4].

Given the stringent regulatory limits imposed on melamine and hydrogen peroxide in milk by food safety authorities worldwide, the fabrication of sensitive and

reliable detection methods is paramount. Plasmonic-based sensing platforms have the potential to address these regulatory requirements while offering advantages such as portability, ease of use, cost-effectiveness and low LOD values. By bridging the gap between fundamental research and practical applications, plasmonic NSs hold promise for revolutionizing food safety monitoring and ensuring the integrity of dairy products in the global market [5,6].

Developing robust and sensitive detection methods for milk adulterants is imperative to ensure food safety and public health [7,8]. Conventional methods like high-performance liquid chromatography (HPLC) [9] and gas chromatography/mass spectrometry (GC/MS) [10] are typically employed to detect adulterants in milk. However, these techniques are highly sophisticated and require trained personnel, making routine screening challenging. Alternative approaches, including aptamer-based sensors [11], quantum dots [12], and colorimetric sensors, have been explored for melamine and hydrogen peroxide detection, but they display high detection limits and provide only qualitative results [13]. While surface enhanced Raman scattering (SERS) technique and electrochemical sensors deem to be promising for detection of these adulterants, but they necessitate laborious sample preparation and sophisticated analysis protocols, limiting their practicality [14,15]. Moreover, these methods may lack the requisite sensitivity to detect adulterants at trace levels, especially in complex matrices like milk. Meanwhile, plasmonic NSs offer a promising avenue for fabrication of sensitive and rapid detection platforms [16]. Their outstanding optical properties, characterized by LSPR, enable label-free detection with high sensitivity and specificity [17]. By harnessing the interaction between the plasmonic NSs and target analytes it is possible to achieve real-time monitoring with minimal sample pretreatment [18]. Furthermore, the tunability of plasmonic NSs allows optimization of sensing performance, including augmented detection limit and selectivity [19,20].

In light of these challenges, the fabrication of a user-friendly, rapid detection method for estimating melamine and hydrogen peroxide content in milk is the need of hour. In the previous chapter, colorimetric sensing methods were investigated for the detection of milk adulterants and contaminants, offering primarily qualitative assessments. Taking cue from this, the current chapter focuses on LSPR-based sensing techniques to

enable the quantitative estimation of adulterant concentrations in milk. It would feasibly enable accurate screening, mitigating the risks associated with adulterated milk consumption and safeguarding public health. Accordingly, this chapter introduces a novel approach for detecting melamine and hydrogen peroxide in raw milk with simplicity and efficiency, eliminating the need for cumbersome NP preparation technique or critical milk pretreatment. The synthesis strategy is meticulously designed to intensify the NPs' selectivity specifically for detecting melamine and hydrogen peroxide as milk adulterants. The resulting sensing platform offers an intuitive, robust, and cost-effective means of quantifying melamine and hydrogen peroxide levels in milk. Through systematic optimization of NP synthesis and surface functionalization, exceptional reproducibility, selectivity, and sensitivity towards their detection via a cost-effective route can be ensured.

3.2 Materials and methods

Ocimum tenuiflorum (OT) (Tulsi) leaves were obtained from Tezpur University Campus, Tezpur, Assam, India. Silver Nitrate ($AgNO_3$) was purchased from Thermo Fisher Scientific. (3-Aminopropyl)-triethoxysilane (≥98.0%) (APTES), Bovine Serum Albumin (BSA), maleic acid (MA), poly vinyl alcohol (PVA), trisodium citrate (TSC), sodium borohydride ($NaBH_4$) and sodium hydroxide (NaOH) was obtained from Merck, USA. Microscopic glass substrate was purchased from a local surgical store was utilised for fabrication of the chip.

Acetone, methanol, and ethanol were obtained from Qualigens and utilised for cleaning purpose. All glass wares and magnetic stirrers used in the synthesis were dipped in freshly prepared aqua regia (HNO_3: HCl; 1:3) overnight and rinsed in distilled water and preserved until dry. Deionized water (DI) and distilled water (DW) were used for synthesis.

3.3 Instrumentation

A UV−Visible spectrophotometer (Thermo Scientific GENESYS 180); an X-ray powder diffractometer (XRD) (D8 FOCUS, Bruker AXS, GERMANY & BRUKER D8 ADVANCE ECO); a Transmission electron microscope (TEM) (Tecnai G2 20 S-TWIN, USA); a Field emission scanning electron microscope (FESEM) (JEOL & GEMINI 500);

Atomic Force Microscopy (AFM) (NTEGRA Vita device from NTMDT & Asylum Research MFP-3D-BIO); a weighing machine (METTLER TOLEDO ME204); a centrifuge machine (Eppendorf 5430R); an oven (Ecogian series; EQUITRON); a tabletop pH meter (EUTECH pH 700), and a magnetic stirrer (SPINOT-TARSONS) were also used during the work.

3.4 LSPR based sensing of melamine by maleic acid functionalised AgNPs

Melamine is a common adulterant added to milk. Its consumption is linked to severe health issues. Despite being banned by multiple regulatory bodies, melamine continues to be used as an adulterant in milk. A significant scandal occurred in China in 2008 due to the widespread consumption of melamine-adulterated milk, highlighting the need for reliable detection methods to prevent such incidents [21,22].

Due to its physical and chemical appearance, melamine is difficult to detect visually in milk. Although sophisticated analytical techniques such as HPLC and other chromatographic methods exist, they are complex and not feasible for routine milk quality monitoring. Some colorimetric detection methods have been reported, but they often fail to provide quantitative estimates of melamine or are unable to detect trace amounts effectively [23-27].

In response to this challenge, researchers like Oh *et al.* developed a cuvette based LSPR sensor for melamine sensing, using a glass chip immobilized with p-nitroaniline-functionalized gold nanoparticles (AuNPs), achieving a LOD of 0.5 ppm [28]. Likewise, Chang *et al.,* also fabricated an LSPR sensor using AuNPs for detection of melamine utilising optical fibre sensing technology, where they obtained a linear response in presence of melamine for concentration range between 0-0.9 μM, while they achieved a LOD of 33 nM. However, fabrication process of these sensors is laborious and quite expensive [29].

To address these limitations, in this part of the chapter, a cuvette-based LSPR sensor has been developed with maleic acid-functionalized AgNPs via a cost-effective route for melamine detection in milk. The core concept behind this approach is the role of maleic acid as a binding agent that facilitates selective interactions with melamine. This binding event induces a measurable shift in the plasmonic spectra, providing a direct indication of melamine presence and enabling precise calibration for quantitative analysis.

3.4.1 Synthesis of maleic acid functionalised AgNPs and pretreatment of milk

Synthesis of maleic acid functionalised AgNPs: The fabrication of the NPs was performed as per the method reported (section 2.B.1.1). For which, 28 mL of 2 mM $NaBH_4$ solution was combined with 12 mL of $AgNO_3$ solution. Then 3 mL of 1% TSC was added dropwise to this solution to properly cap the NPs and prevent it from aggregating [30].

For the functionalization of NPs, method reported in section 2.B.1.1 was followed. 2 mL of a 1 mM maleic acid solution was added to the NP solution, followed by stirring for 10 minutes at 600 rpm. Subsequently, the pH of the solution was brought to 7 through the addition of NaOH [31].

Pretreatment of milk: Same protocol was implemented as outlined in the previous study (section 2.A.1.1). After following this process, the resultant milk supernatant, was then spiked with various concentrations of melamine (1 to 100 ppb) for subsequent testing.

3.4.2 Characterisation of maleic acid functionalised AgNPs

The UV-Vis, XRD, and TEM characterisation of the synthesised NPs has already been discussed in the section 2.B.2.1 of chapter 2 of the thesis [32,33].

FESEM analysis was also done to scrutinize the morphological characteristics of the synthesized NPs on the plasmonic chip. In this process, the fabricated LSPR sensor was meticulously sliced into dimensions of area 0.5 cm^2 and subsequently spin-coated for enhanced visualization. The mean diameter of these NPs was estimated to be approximately 24 nm, where each particle ranges between 12 nm and 38 nm. Moreover,

the NPs were of uniform size and shape and were well distributed on the substrate (**Fig. 3.1.a**) [34,35].

AFM analysis was also conducted following a protocol similar to that for FESEM analysis, albeit with glass slides cut to dimensions of 1 cm × 1 cm. The AFM results unveiled a homogeneous distribution of NPs across the surface of the glass chip. Furthermore, a profile analysis was performed to determine the thickness of the NP distribution, revealing a range between 5 to 20 nm. Remarkably, this thickness aligns closely with the size of the synthesized NPs as affirmed by TEM and FESEM studies. This consistency suggests the presence of a thin, single-layered NP coating on the glass surface, ensuring the precision and uniformity achieved in the NP deposition process (**Fig. 3.1.b; Fig. 3.1.c & Fig. 3.1.d**) [36].

3.4.3 LSPR based plasmonic sensing

3.4.3.1 Fabrication of the sensor

The glass substrate (measuring 0.8 cm in width and 5 cm in length) of the LSPR sensor underwent a thorough cleaning process to ensure optimal surface conditions. Initially, it was immersed in methanol, followed by a 20-min sonication period, and rinsed subsequently four times with DW to completely eliminate any residual methanol. Next, the substrate was treated with APTES by immersing it in a 0.5% APTES solution for 1 h at 50°C to facilitate effective functionalization on its surface [28,37,38].

In the next step, the glass substrate underwent five additional rinses with DW to remove any excess unbound APTES on the surface of the glass slide. It was then immersed in a solution of MA-functionalised AgNPs for 16 h, allowing the MA-AgNPs to self-assemble into a single layer on the substrate [28,38,39].

Following the immobilization of NPs on the surface of the glass substrate, the decorated glass slides were washed multiple times with DW to eliminate any unbound particles residing on its surface. Subsequently, the plasmonically active chip was immersed in a 1% solution of BSA for 30 min to effectively encapsulate the LSPR chip (**Fig.3.2**) [28,37].

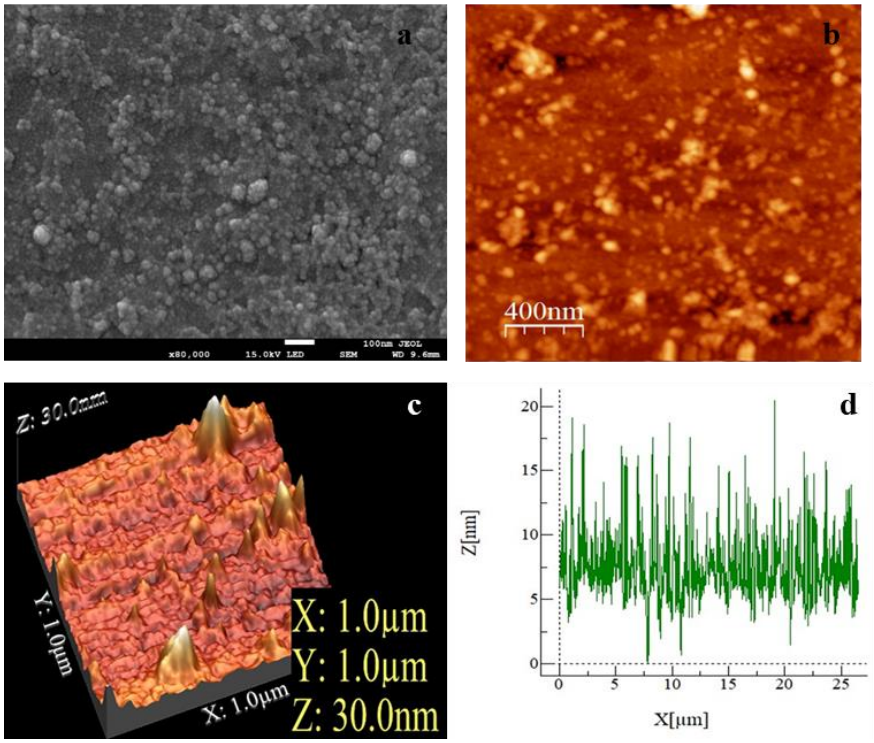

Figure 3.1: *Characterisation of MA-AgNPs* ***(a)*** *FESEM image,* ***(b)*** *AFM image (2D representation),* ***(c)*** *AFM image (3D representation), and* ***(d)*** *size distribution profile of MA-AgNP across the LSPR chip.*

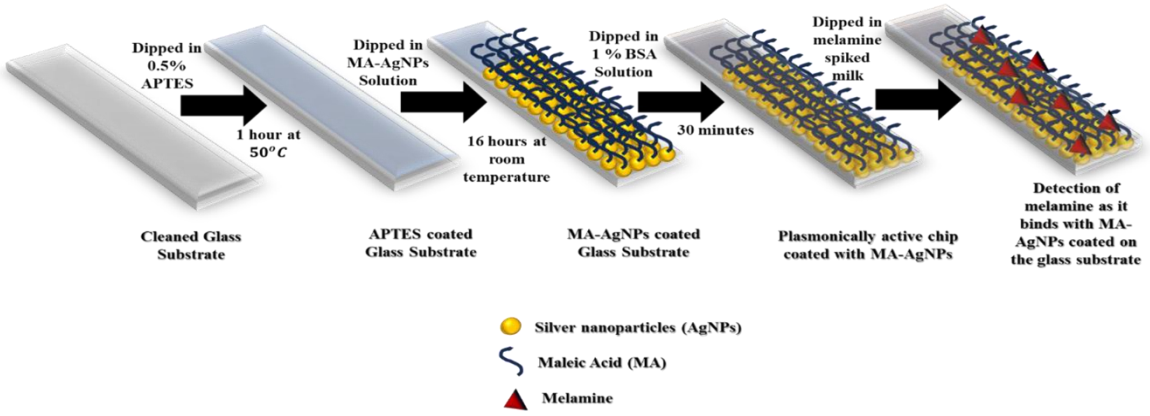

Figure 3.2: *Schematic representation of fabrication of the MA-AgNPs LSPR chip.*

3.4.3.2 Mechanism

The maleic acid compound, possessing two carboxylic groups, exhibits a unique structural configuration conducive to facile binding onto the surface of bare NPs. Its interaction with melamine, rich in amine groups, is orchestrated by hydrogen bonding. Specifically, the hydrogen of the amine group in melamine bonds with the maleic acid attached to the NP surface. This hydrogen bonding involves the oxygen atom of the maleic acid group

interacting with the hydrogen atom of the amine group in melamine. Again, melamine contains three amine group where each group contains two hydrogens interacting with maleic acid. Consequently, this interaction induces alterations in the refractive index of the surrounding medium which alters the position of the plasmonic band [28,40,41].

In the experiment, the maleic acid-functionalized AgNPs were initially immobilized onto a glass substrate using APTES as a coupling agent. Upon exposure to a milk solution containing melamine, the surface functionalization facilitated interactions with the three amine groups of melamine which yielded a discernible red shift in the plasmonic peak (**Fig. 3.3**).

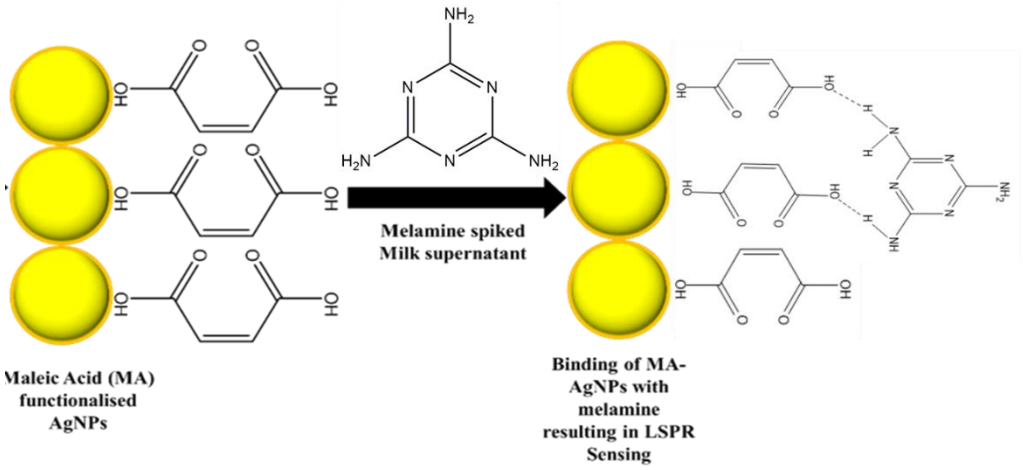

Figure 3.3: *Pictorial representation of detection mechanism for sensing of melamine in milk.*

3.4.3.3. Selectivity study

Furthermore, selective study was performed to evaluate the susceptibility of the detection process due to interference from alternative adulterants, via UV-vis analysis. Intriguingly, the analysis revealed that only melamine induced a discernible shift in the absorbance peak at 10 ppb, while other adulterants such as formalin, urea, hydrogen peroxide, ammonium sulphate, cyanuric acid and salicylic acid exhibited minimal influence at 50 ppb concentration in each milk supernatant. Notably, melamine demonstrated the most pronounced response in terms of peak shift compared to its counterparts present in milk. This significant observation underscores the efficacy of the functionalized NPs in facilitating the precise and selective detection of melamine in milk samples (**Fig. 3.4**) [28].

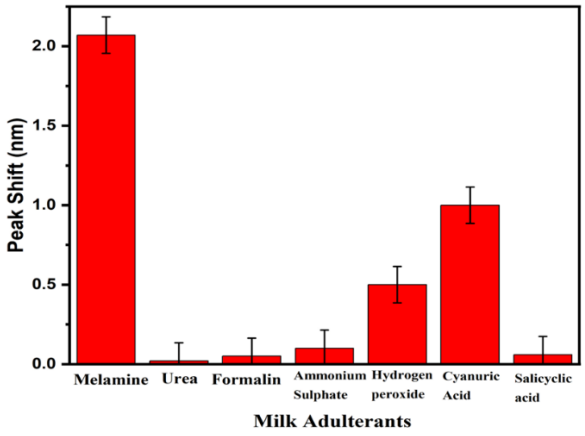

Figure 3.4: *Histogram plot of selectivity test in the presence of various adulterants.*

3.4.3.4 Sensor performance metrics

With increase in concentration of melamine in milk supernatant, a significant shift in the plasmonic spectra was obtained as evinced in the UV-Vis spectra. Following which, a linear correlation was established between the observed peak shift and melamine concentration leading to a calibration graph. This graph was then used for determination of LOD which was found to be 10.48 ppb. This was calculated based on the standard deviation of blank and slope of the calibration graph. Utilising the formula, $\frac{3.3\sigma}{s}$ (Where, σ refers to standard deviation of blank measurements (n = 3) and s refers the slope of calibration graph) (as reported in equation 2.A.1.). Importantly, the LOD emphasized the heightened sensitivity of the developed sensing platform, surpassing the stringent limits prescribed by governmental regulatory agencies. The sensor displayed a dynamic sensing range spanning from 10 to 50 ppb, showcasing its capability to detect melamine even at lower concentrations. The system's sensitivity, quantified as 0.11 nm/ ppb, ensures its ability to discern minute changes in melamine concentration with high precision (**Fig. 3.5**) [28,42].

Furthermore, the recovery efficiency of the fabricated device was assessed which yielded values between 96%-99.4%. Thus, demonstrating its robustness and repeatability in analytical measurements [43].

This experimental setup can also be used for the quantification of melamine in milk. To validate this, several experiments were conducted to assess the error associated with the

calibrated graphs. The error ranged from 0.8% to 4%, indicating that the fabricated sensor is capable of providing accurate quantitative assessments of melamine in milk. The process involves first measuring the peak shift value, which, when applied to the linear calibration equation, yields the melamine concentration with high accuracy and minimal error. This enables precise quantitative analysis of melamine, even at trace levels, in milk samples (**Table 3.1**)

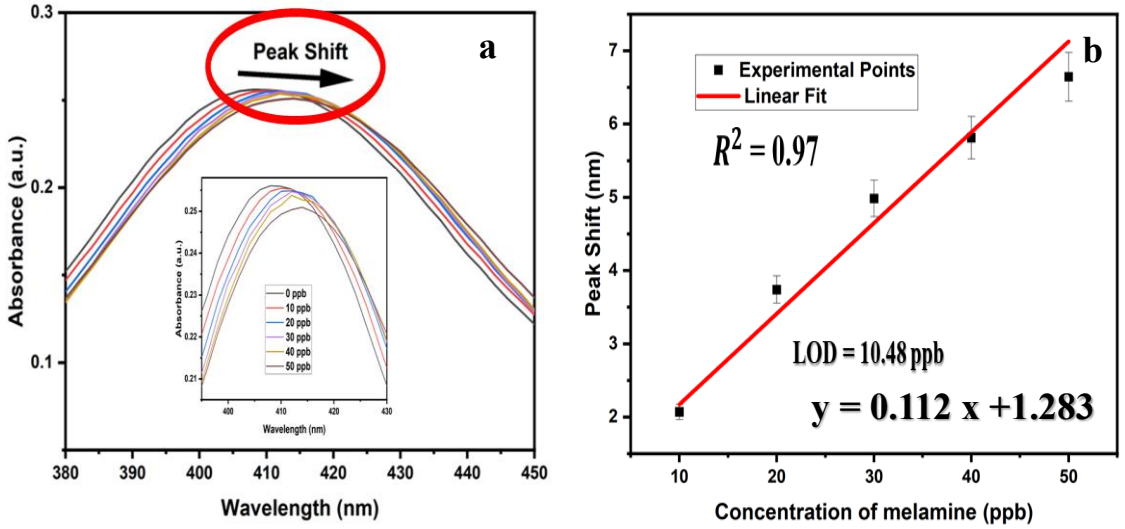

Figure 3.5: (a) *UV-Vis plots depicting plasmonic peak shift with changing concentrations of melamine in milk, and* ***(b)*** *calibration plot between peak shift vs. concentration of melamine.*

Table 3.1: *Quantitative estimation of melamine in milk.*

SL. No.	Peak Shift (y) (nm)	Theoretical value of concentration (x_0) (ppb)	Experimental value of concentration (x) (ppb)	Error % $(\frac{x_0-x}{x_0} \times 100)$
1	1.82	5	4.8	4
2	2.918	15	14.6	2.6
3	4.027	25	24.5	2
4	5.18	35	34.8	0.57
5	6.278	45	44.6	0.8

3.5 LSPR based Sensing of Hydrogen Peroxide by PVA functionalised *Ocimum tenuiflorum* leaves reduced AgNPs*

Hydrogen peroxide is an illegal milk adulterant occasionally used to inhibit microbial growth and extend shelf life. While it is effective at reducing spoilage, its use poses significant health risks due to its oxidative properties. Ingestion of hydrogen peroxide, especially in large quantities, can lead to gastrointestinal irritation, tissue damage, and oxidative stress, which may result in serious complications such as skin disorders, liver damage, and other health issues [44,45].

Plasmonic sensing principles offer a powerful tool for detecting hydrogen peroxide adulteration, even in trace amounts, below permissible limits. Hydrogen peroxide, as a strong oxidizing agent, binds with NPs in the sensor. This binding alters the local refractive index, and due to its strong oxidizing nature, it causes a reduction in the number of NPs, along with alteration of their shape and size. These changes induce a measurable shift in the plasmonic peak, which can be quantified to estimate the amount of hydrogen peroxide present in the milk [46,47].

In literature, there are certain methods such as colorimetric method, chromatographic analysis, florescent and electrochemical methods available to detect the toxic adulterants. Even though these methods are highly advanced and sophisticated, some of them could not even detect trace amount of it in milk making it necessary to fabricate a user-friendly device which could be used for on spot and real time assessing the quality of milk. Here in, plasmonic optical sensor comes as a saviour [48,49].

Recently, a notable study by Semwal *et al.* developed a SPR-based sensor using fibre optic technology to detect hydrogen peroxide. The sensing probe was created by coating Au and graphene oxide (GO) on an unclad optical fibre core and it was covered with immobilized catalase enzyme. Au was used to enhance the stability of the sensor. While GO improved its sensitivity; catalase provided high specificity for hydrogen peroxide detection. This sensor achieved a LOD of 55 μM. However, the fabrication process of this sensor was complex, requiring multiple chemicals and intricate techniques [50].

*This section of the thesis is published in U Das *et al.*, *ACS Omega*, 10(21), 2025

Taking cue of these facts, an attempt was made to fabricate an LSPR-based hydrogen peroxide sensor using glass as the substrate. In this approach, AgNPs were synthesized using *Ocimum tenuiflorum* (OT) leaves extract, which acted as a strong reducing agent to facilitate the formation of NPs. These synthesized NPs were immobilized on glass slides and then coated with PVA as a functionalising element. When exposed to hydrogen peroxide, the immobilized NPs interacted with the adulterant, causing a decrease in the absorbance peak with a shift in the plasmonic peak. This shift was calibrated to accurately estimate the amount of hydrogen peroxide in milk, allowing sensitive detection of the adulterant, even at trace levels. This method not only simplifies the sensor fabrication process but also provides a reliable approach for monitoring hydrogen peroxide in milk.

3.5.1 Synthesis of PVA functionalised AgNPs and pretreatment of milk

Synthesis of reducing, functionalising agent and the precursor: 10 mM $AgNO_3$ solution was prepared by adding 0.169 g to 100 mL of DW, which was stirred at room temperature for a duration of 10 min at a rate of 600 rpm.

Following which, the tulsi leaves extract was prepared. Accordingly, 5 g of tulsi leaves were chopped into small pieces, properly washed and kept in an oven to dry at 80^{o}C for 2 h. These dried tulsi leaves were crushed and added to 100 mL of DW. The resulting mixture was heated at 100^{o}C for 2 h. Then, this extract was filtered twice by using Whatman filter paper no. 1 [51].

For functionalisation of NPs, 1% PVA solution was prepared for which 1 g of PVA was added to 100 mL of DW and dissolved by stirring it at 60^{o}C for a duration of 3 h at a rate of 700 rpm.

Preparation of functionalised AgNPs: 40 mL of 10 mM $AgNO_3$ solution was stirred continuously to which 5 mL of tulsi leaves extract was added dropwise and the resulting solution was stirred at 700 rpm at 80^{o}C for a duration of 30 min. The colour of the solution slowly changed to yellow indicating formation of NPs in the solution. The pH of the solution was then adjusted to 7 by adding 0.1 M NaOH solution under continuous stirring

at 700 rpm. The yellow colour of the resulting solution indicated formation of AgNPs [51,52].

Pretreatment of milk: Same protocol was implemented as outlined in the previous study (section 2.A.1.1). After following this process, the resultant milk supernatant, was then spiked with various concentrations of hydrogen peroxide (1 to 100 ppb) for subsequent testing

3.5.2 Characterisation of PVA functionalised AgNPs

Characterisation of the NPs were performed by following the previous protocol. UV–Vis analysis was performed where the NPs displayed an intense broad absorption peak at 434 nm. The obtained broad peak indicated polydisperse nature of the synthesised NPs (**Fig. 3.6.a**) [32].

In XRD spectra, four distinct peaks were observed at 38.56°, 44.56°, 64.71°, and 77.75°, corresponding to the diffraction planes (111), (200), (220), and (311) of silver, which confirms FCC crystalline nature of synthesised AgNPs (**Fig. 3.6.b**) [33].

FESEM images revealed the mean size of the NPs to be approximately 30 nm, where each particle ranges between 10 nm and 40 nm (**Fig. 3.6.c**) [34]. Likewise, TEM analysis confirmed that the synthesised NPs were of size approximately, 19.47 nm, with particle sizes spanning between 3 and 45 nm. Moreover, the morphological examination depicted a predominantly spherical configuration (**Fig. 3.6.d; Fig. 3.6.e** & **Fig. 3.6.f**) [35].

AFM analysis was also conducted following a protocol similar as discussed in the earlier section. The results unveiled a homogeneous distribution of a thick layer of NPs across the surface of the glass chip. Furthermore, a profile analysis was performed to determine the thickness of the NP distribution, revealing a range between 5 to 170 nm. This consistency suggests the presence of a thick, triple-layered NP along with PVA capping on the chip surface, underscoring the precision and uniformity achieved in the NP deposition process for the subsequent application (**Fig. 3.6.g; Fig. 3.6.h** & **Fig. 3.6.i**) [36].

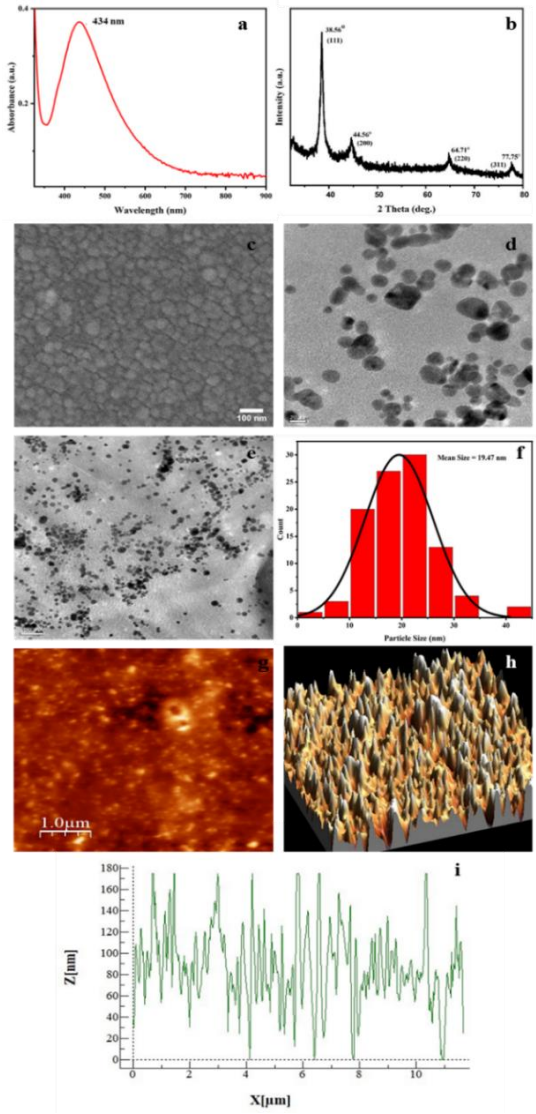

Figure 3.6: *Characterisation of PVA-AgNPs* ***(a)*** *UV-Vis spectrum,* ***(b)*** *XRD pattern,* ***(c)*** *FESEM image,* ***(d)*** *TEM image (under high magnification),* ***(e)*** *TEM image (under low magnification),* ***(f)*** *Size distribution analysis from TEM,* ***(g)*** *AFM image (2D representation),* ***(h)*** *AFM image (3D representation), and* ***(i)*** *Size distribution profile of PVA-AgNPs across the LSPR chip.*

3.5.3 LSPR based plasmonic sensing

3.5.3.1 Fabrication of the sensor

Cleaning and preparation of the glass slides were performed as per the protocol reported (section 3.4.3.1) [28]. Next, the substrate was immersed in a 1% solution of APTES and treated at 60°C for 1 h, effectively functionalizing its surface [28].

Afterward, the glass substrate underwent five additional rinses with DW to remove any excess APTES solution. It was then immersed in a solution of tulsi leaves reduced AgNPs for 24 h, allowing the NPs to self-assemble into a thick layer on the substrate. Following which the immobilised NPs coated glass substrate was dipped in 1 % PVA solution for 1 h [28,37,38].

Following the immobilization of NPs on the glass substrate, the substrate was washed multiple times with DW to eliminate any unbound particles residing on its surface. Subsequently, the plasmonically active chip was immersed in a 1% solution of BSA for 30 min to effectively encapsulate the LSPR chip (**Fig. 3.7**) [28].

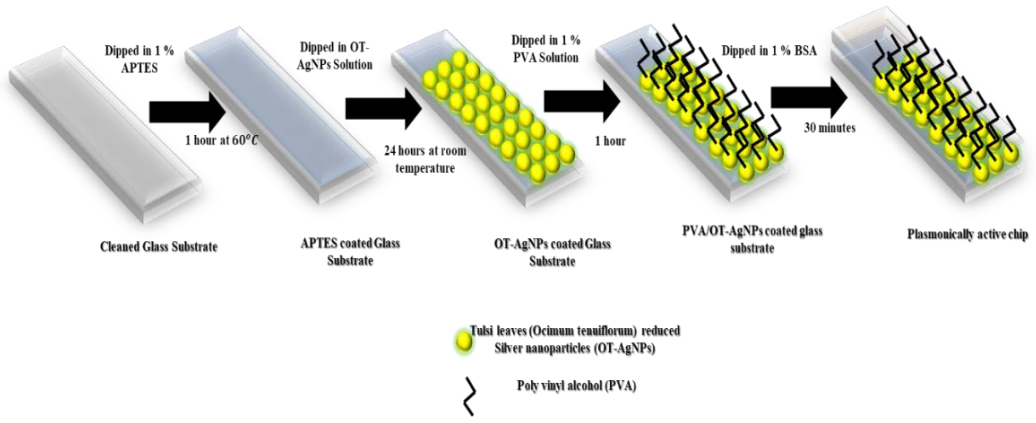

Figure 3.7: *Schematic representation of fabrication of the PVA-AgNPs LSPR sensor.*

3.5.3.2 Mechanism

Tulsi leaves are rich in active antioxidants, such as polyphenols and flavonoids, which play a pivotal role in reducing silver ions (Ag^{+}) to form AgNPs. During this reduction process, the polyphenols and phytochemicals in the leaf extract not only facilitate NP synthesis but also serve as capping agents—thereby stabilizing the NPs and preventing their aggregation by encapsulating their surface [53,54].

Once synthesized, the AgNPs are immobilized onto a glass substrate, forming a stable and uniform plasmonic nanofilm for sensing applications. To improve film stability and prevent NP aggregation, the surface of the AgNPs was coated with PVA. The PVA matrix serves a dual role: it anchors the AgNPs firmly onto the glass surface while

providing a hydrophilic environment that facilitates the diffusion of hydrogen peroxide molecules toward the NPs [55,56].

Upon exposure to hydrogen peroxide, direct interaction occurs at the AgNP surface. This interaction may be through simple hydrogen bonding with the hydroxyl groups of PVA. Since hydrogen peroxide is a strong oxidizing agent, it partially oxidizes the metallic Ag^0 surface atoms of the NPs to Ag^+. This surface oxidation induces subtle but significant alterations in NP morphology, and the local dielectric environment. These physicochemical changes disrupt the equilibrium of localized surface plasmons and result in a measurable shift in the LSPR absorption peak.

The magnitude of this plasmonic shift was directly related to the extent of AgNP surface modification, which in turn depends on the concentration of hydrogen peroxide present [57,58] (**Fig. 3.8**).

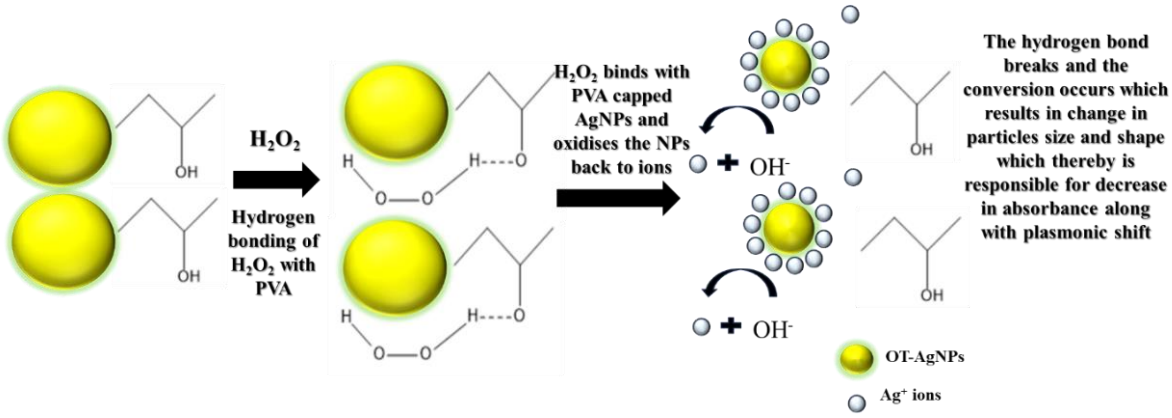

Figure 3.8: *Pictorial representation of detection mechanism for sensing of hydrogen peroxide in milk.*

3.5.3.3 Selectivity study

In similitude to the other works, a selective analysis was performed employing UV-Vis analysis to evaluate the susceptibility of the detection process due to interference from alternative adulterants such as urea, melamine, dextrose, ammonium phosphate and formalin. Milk samples were spiked with 225 ppb concentration of each adulterant and 45 ppb concentration of hydrogen peroxide to perform the selectivity test. Intriguingly, the analysis revealed that only hydrogen peroxide induced a significant shift in the absorbance peak, while other adulterants exhibited very minimal influence. This is because other adulterants do not interfere with the encapsulated NPs and thus, do not cause any

significant shift in the LSPR band of the AgNPs. Notably, hydrogen peroxide demonstrated the most pronounced response in terms of peak shift compared to its counterparts present in milk. This significant observation underscores the efficacy of the functionalized NPs in facilitating the precise and selective detection of hydrogen peroxide within milk samples (**Fig. 3.9**).

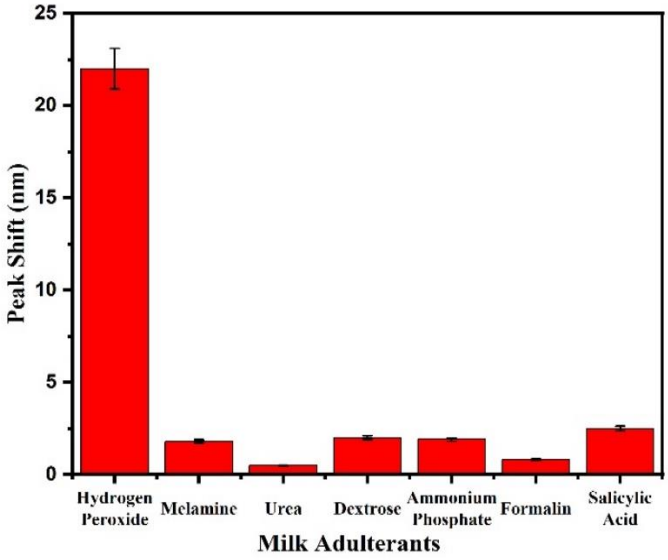

Figure 3.9: *Histogram plot representing selectivity test in the presence of various adulterants.*

3.5.3.4 Sensor performance metrics

The UV-Vis absorbance spectrum displayed a substantial decrease in absorbance along with shift in the plasmonic peak corresponding to increment in concentration of hydrogen peroxide in milk. A linear correlation was established between the observed peak shift/ decrease in absorbance and with increase in amount of hydrogen peroxide. This graph enabled the determination of the LOD which has been found to be 2.72 ppb (this was obtained by using the formula 2.A.1) [59,60]. Notably, this value highlights the exceptional sensitivity of the developed sensing platform, exceeding the stringent limits established by regulatory agencies. The sensor demonstrated a dynamic detection range of 1 to 45 ppb, with a sensitivity of 0.46 nm/ppb change in concentration of hydrogen peroxide, reflecting its capability to detect even trace amount of hydrogen peroxide concentration with remarkable precision (**Fig. 3.10**) [60].

Furthermore, the recovery efficiency of the fabricated device was assessed, and it emerged as 97%-108%. This highlights the sensor's reliability and reproducibility to detect hydrogen peroxide in milk supernatant with higher accuracy [61].

This experimental setup can also be utilized for the quantification of amount of hydrogen peroxide in milk. To validate this, several experiments were conducted to assess the error associated with the calibrated graphs. The error ranged from 1.33% to 8%, indicating that the fabricated sensor system can provide accurate quantitative assessments of hydrogen peroxide concentration in milk. The process entails measuring the peak shift value, which was then applied to the linear calibration equation to accurately determine the hydrogen peroxide concentration with minimal error. This enables precise quantitative analysis of hydrogen peroxide, even at trace levels, in milk samples (**Table 3.2**).

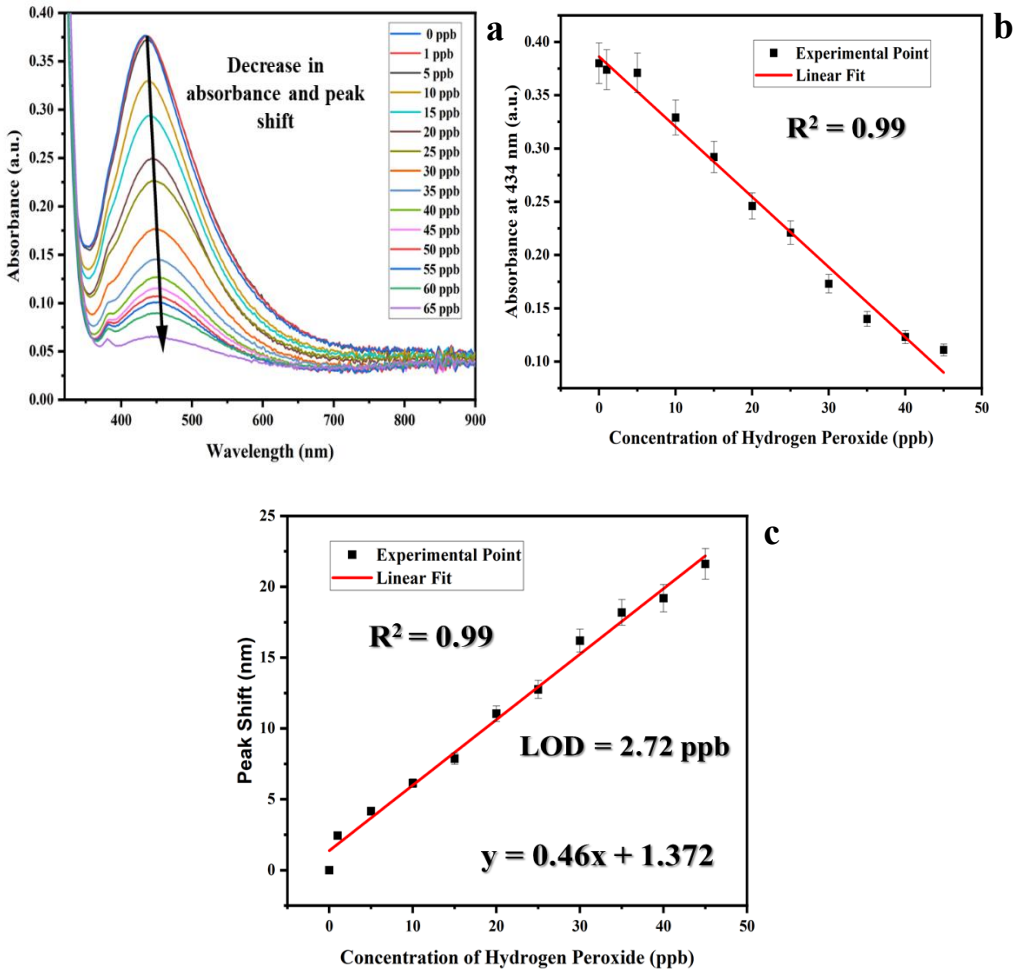

Figure 3.10: (a) *UV-Vis plots depicting peak shift and decrease in absorbance with changing concentrations of hydrogen peroxide in milk, calibration plot between* ***(b)*** *absorbance vs. concentration of hydrogen peroxide, and* ***(c)*** *peak shift vs. concentration of hydrogen peroxide.*

Table 3.2: *Quantitative estimation of hydrogen peroxide in milk.*

Sl. no.	Peak Shift (y) (nm)	Theoretical value of concentration (x_o) (ppb)	Experimental value of concentration (x) (ppb)	Error % $(\frac{x_0-x}{x_0} \times 100)$
1	2.61	2.5	2.7	8.00
2	4.78	7.5	7.4	1.33
3	6.98	12.5	12.2	2.40
4	9.61	17.5	17.9	2.28
5	12.04	22.5	23.2	3.11

3.6 Conclusion

This study reports the fabrication of a highly selective and sensitive plasmonic sensor for detection of melamine and hydrogen peroxide in milk, representing a significant advancement in food safety monitoring. Utilizing comprehensive characterization techniques such as UV-Vis spectroscopy, XRD, TEM, FESEM, and AFM, the optical, structural, and morphological properties of the synthesized NPs were elucidated. NPs functionalised with maleic acid and PVA, exhibited a strong affinity for the target analyte melamine and hydrogen peroxide, respectively. This led to the distinct plasmonic peak shifts as confirmed by UV-Vis spectroscopy. The sensor demonstrated exceptional performance, with LOD as low as 10.48 ppb for melamine and 2.72 ppb for hydrogen peroxide, surpassing the stringent thresholds set by regulatory agencies. Recovery efficiency of 96%-99.4% and 97%-108% for melamine and hydrogen peroxide, respectively shows the reliability of the system for repeated and quantitative measurements. Additionally, the innovative design, leveraging LSPR technology, offers high reproducibility and real-world applicability. Overall, this LSPR-based sensor offers a user-friendly, eco-friendly, and highly accurate solution for on-site milk quality monitoring. Its robust performance and simplicity in fabrication position it as a promising tool for combating milk adulteration.

References

[1] Khan, I., Saeed, K., and Khan, I. Nanoparticles: Properties, applications and toxicities. *Arabian journal of chemistry*, 12(7): 908-931, 2019.

[2] Xu, Y., Bai, P., Zhou, X., Akimov, Y., Png, C. E., Ang, L. K., Knoll, W., and Wu, L. Optical refractive index sensors with plasmonic and photonic structures: promising and inconvenient truth. *Advanced Optical Materials*, 7(9): 1801433, 2019.

[3] Ritota, M., and Manzi, P. Melamine detection in milk and dairy products: traditional analytical methods and recent developments. *Food analytical methods*, 11: 128-147, 2018.

[4] Rysstad, G., and Kolstad, J. Extended shelf-life milk—advances in technology. *International journal of dairy technology*, 59(2): 85-96, 2006.

[5] Balbinot, S., Srivastav, A. M., Vidic, J., Abdulhalim, I., and Manzano, M. Plasmonic biosensors for food control. *Trends in Food Science & Technology*, 111: 128-140, 2021.

[6] Putri, L. A., Prabowo, Y. D., Dewi, D. M. M., Mumtazah, Z., Adila, F. P., Fadillah, G., Amrillah, T., Triyana, K., Nugroho, F. A. A., and Wasisto, H. S. Review of Noble Metal Nanoparticle-Based Colorimetric Sensors for Food Safety Monitoring. *ACS Applied Nano Materials*, 7(17): 19821-19853, 2024.

[7] Abedini, R., Khaniki, G. J., Naderi, M., Aghaee, E. M., and Sadighara, P. Investigation of melamine and cyanuric acid concentration in several brands of liquid milk and its non-carcinogenic risk assessment in adults and infants. *Journal of Food Science and Technology*, 60(12): 3054-3066, 2023.

[8] Abbas, M. E., Luo, W., Zhu, L., Zou, J., and Tang, H. Fluorometric determination of hydrogen peroxide in milk by using a Fenton reaction system. *Food chemistry*, 120(1): 327-331, 2010.

[9] Abedini, R., Jahed Khaniki, G., Molaee Aghaee, E., Sadighara, P., Nazmara, S., Akbari-Adergani, B., and Naderi, M. Determination of melamine contamination in chocolates containing powdered milk by high-performance liquid chromatography (HPLC). *Journal of Environmental Health Science and Engineering*, 19: 165-171, 2021.

[10] Xu, X. M., Ren, Y. P., Zhu, Y., Cai, Z. X., Han, J. L., Huang, B. F., and Zhu, Y. Direct determination of melamine in dairy products by gas chromatography/mass spectrometry with coupled column separation. *Analytica Chimica Acta*, 650(1): 39-43, 2009.

[11] Kaneko, N., Horii, K., Akitomi, J., Kato, S., Shiratori, I., and Waga, I. An aptamer-based biosensor for direct, label-free detection of melamine in raw milk. *Sensors*, 18(10): 3227, 2018.

[12] Lv, J., Liu, S., and Miao, Y. Synthesis of biological quantum dots based on single-strand DNA and its application in melamine detection. *Spectrochimica Acta Part A: Molecular and Biomolecular Spectroscopy*, 248: 119254, 2021.

[13] Paul, I. E., Rajeshwari, A., Prathna, T. C., Raichur, A. M., Chandrasekaran, N., and Mukherjee, A. Colorimetric detection of melamine based on the size effect of AuNPs. *Analytical Methods*, 7(4): 1453-1462, 2015.

[14] Cheng, J., Su, X. O., Yao, Y., Han, C., Wang, S., and Zhao, Y. Highly sensitive detection of melamine using a one-step sample treatment combined with a portable Ag nanostructure array SERS sensor. *PLoS One*, 11(4): e0154402, 2016.

[15] An, Q. Q., Feng, X. Z., Zhou, Z. F., Zhan, T., Lian, S. F., Zhu, J., Han, G. C., Chen, Z., and Kraatz, H. B. One step construction of an electrochemical sensor for melamine detection in milk towards an integrated portable system. *Food Chemistry*, 383: 132403, 2022.

[16] Haque, M. A., Rahad, R., Rakib, A. K. M., Sharar, S. S., and Sagor, R. H. Plasmonic sensor for rapid detection of water adulteration in honey and quantitative measurement of lactose concentration in solution. *Results in Physics*, 51: 106733, 2023.

[17] Peltomaa, R., Glahn-Martínez, B., Benito-Peña, E., and Moreno-Bondi, M. C. Optical biosensors for label-free detection of small molecules. *Sensors*, 18(12): 4126, 2018.

[18] D'Agata, R., Bellassai, N., and Spoto, G. Exploiting the design of surface plasmon resonance interfaces for better diagnostics: A perspective review. *Talanta*, 266: 125033, 2024.

[19] Acunzo, A., Scardapane, E., De Luca, M., Marra, D., Velotta, R., and Minopoli, A. Plasmonic nanomaterials for colorimetric biosensing: a review. *Chemosensors*, 10(4): 136, 2022.

[20] Hill, R. T. Plasmonic biosensors. *Wiley Interdisciplinary Reviews: Nanomedicine and Nanobiotechnology*, 7(2): 152-168, 2015.

[21] Skinner, C. G., Thomas, J. D., and Osterloh, J. D. Melamine toxicity. *Journal of Medical Toxicology*, 6: 50-55, 2010.

[22] Wang, Q., Wei, L., and Wang, W. Challenges and prospects for milk production in China after the 2008 milk scandal. *Applied Animal Science*, 37(2): 166-175, 2021.

[23] Liu, Y., Todd, E. E., Zhang, Q., Shi, J. R., and Liu, X. J. Recent developments in the detection of melamine. *Journal of Zhejiang University Science B*, 13(7): 525-532, 2012.

[24] Venkatasami, G., and Sowa Jr, J. R. A rapid, acetonitrile-free, HPLC method for determination of melamine in infant formula. *Analytica Chimica Acta*, 665(2): 227-230, 2010.

[25] Wu, Z., Zhao, H., Xue, Y., Cao, Q., Yang, J., He, Y., ... and Yuan, Z. Colorimetric detection of melamine during the formation of gold nanoparticles. *Biosensors and Bioelectronics*, 26(5): 2574-2578, 2011.

[26] Paul, I. E., Rajeshwari, A., Prathna, T. C., Raichur, A. M., Chandrasekaran, N., and Mukherjee, A. Colorimetric detection of melamine based on the size effect of AuNPs. *Analytical Methods*, 7(4): 1453-1462, 2015.

[27] Xing, H., Zhan, S., Wu, Y., He, L., and Zhou, P. Sensitive colorimetric detection of melamine in milk with an aptamer-modified nanogold probe. *RSC advances*, 3(38): 17424-17430, 2013.

[28] Oh, S. Y., Lee, M. J., Heo, N. S., Kim, S., Oh, J. S., Lee, Y., Jeon, E. J., Moon, H., Kim, H. S., Park, T. J., Moon, G., Chun, H. S., and Huh, Y. S. Cuvette-type LSPR sensor for highly sensitive detection of melamine in infant formulas. *Sensors*, 19(18): 3839, 2019.

[29] Chang, K., Wang, S., Zhang, H., Guo, Q., Hu, X., Lin, Z., Lin, Z., Sun, H., Jiang, M., and Hu, J. Colorimetric detection of melamine in milk by using gold nanoparticles-based LSPR via optical fibers. *PLoS One*, 12(5): e0177131, 2017.

[30] Sholikhah, U., Pujiyanto, A., Lestari, E., Sarmini, E., and Lubis, H. Critical parameters of silver nanoparticles (AgNPs) synthesized by sodium borohydride reduction. *Research Journal of Chemical and Environmental Sciences*, 22(2): 179-183, 2018.

[31] Boruah, B. S., Daimari, N. K., and Biswas, R. Functionalized silver nanoparticles as an effective medium towards trace determination of arsenic (III) in aqueous solution. *Results in Physics*, 12: 2061-2065, 2019.

[32] Sholikhah, U. N., Pranowo, D., Arvianto, R. I., Sarmini, E., and Widyaningrum, T. Purification Method of Silver Nanoparticles (AgNPs) and its Identification Using UV-Vis Spectrophotometer. *Key Engineering Materials*, 840: 484-491, 2020.

[33] Babu, S. A., and Prabu, H. G. Synthesis of AgNPs using the extract of Calotropis procera flower at room temperature. *Materials Letters*, 65(11): 1675-1677, 2011.

[34] Karumuri, A. K., Maleszewski, A. A., Oswal, D. P., Hostetler, H. A., and Mukhopadhyay, S. M. Fabrication and characterization of antibacterial nanoparticles

supported on hierarchical hybrid substrates. *Journal of nanoparticle research*, 16: 1-14, 2014.

[35] Babu, S. A., and Prabu, H. G. Synthesis of AgNPs using the extract of Calotropis procera flower at room temperature. *Materials Letters*, 65(11): 1675-1677, 2011.

[36] Teerasong, S., Sani, M., Numsawat, P., Martchoo, R., Chompoosor, A., and Nacapricha, D. A silver nanoparticle thin film modified glass substrate as a colourimetric sensor for hydrogen peroxide. *Journal of Experimental Nanoscience*, 10(17): 1327-1335, 2015.

[37] Oh, S. Y., Heo, N. S., Bajpai, V. K., Jang, S. C., Ok, G., Cho, Y., and Huh, Y. S. Development of a cuvette-based LSPR sensor chip using a plasmonically active transparent strip. *Frontiers in bioengineering and biotechnology*, 7: 299, 2019.

[38] Jung, D., Ahn, J., Jo, N., Lee, J., Shin, Y. B., and Lim, H. Cuvette-based microfluidic device integrated with nanostructures for measuring dual Localized Surface Plasmon Resonance (LSPR) signals. *Review of Scientific Instruments*, 89(11): 2018.

[39] Fernández, F., Garcia-Lopez, O., Tellechea, E., Asensio, A. C., and Cornago, I. LSPR Cuvette for Real-Time Biosensing by using a common spectrophotometer. *IEEE Sensors Journal*, 16(11): 4158-4165, 2016.

[40] Farrokhnia, M., Karimi, S., and Askarian, S. Strong hydrogen bonding of gallic acid during synthesis of an efficient AgNPs colorimetric sensor for melamine detection via dis-synthesis strategy. *ACS Sustainable Chemistry & Engineering*, 7(7): 6672-6684, 2019.

[41] Zhang, X., Zhao, H., Xue, Y., Wu, Z., Zhang, Y., He, Y., Li, X., and Yuan, Z. Colorimetric sensing of clenbuterol using gold nanoparticles in the presence of melamine. *Biosensors and Bioelectronics*, 34(1): 112-117, 2012.

[42] Chen, W., Deng, H. H., Hong, L., Wu, Z. Q., Wang, S., Liu, A. L., Linab X. H., and Xia, X. H. Bare gold nanoparticles as facile and sensitive colorimetric probe for melamine detection. *Analyst*, 137(22): 5382-5386, 2012.

[43] Liu, X., Wang, J., Wang, Y., Huang, C., Wang, Z., and Liu, L. In situ functionalization of silver nanoparticles by gallic acid as a colorimetric sensor for simple sensitive determination of melamine in milk. *ACS omega*, 6(36): 23630-23635, 2021.

[44] Munro, I. C., Williams, G. M., Heymann, H. O., and Kroes, R. Use of hydrogen peroxide-based tooth whitening products and its relationship to oral cancer. *Journal of esthetic and restorative dentistry*, 18(3): 119-125, 2006.

[45] Pravda, J. Hydrogen peroxide and disease: towards a unified system of pathogenesis and therapeutics. *Molecular Medicine*, 26(1): 41, 2020.

[46] Vasileva, P., Donkova, B., Karadjova, I., and Dushkin, C. Synthesis of starch-stabilized silver nanoparticles and their application as a surface plasmon resonance-based sensor of hydrogen peroxide. *Colloids and Surfaces A: Physicochemical and Engineering Aspects*, 382(1-3): 203-210, 2011.

[47] Teodoro, K. B., Migliorini, F. L., Christinelli, W. A., and Correa, D. S. Detection of hydrogen peroxide (H2O2) using a colorimetric sensor based on cellulose nanowhiskers and silver nanoparticles. *Carbohydrate polymers*, 212: 235-241, 2019.

[48] Zhang, L., and Li, L. Colorimetric detection of hydrogen peroxide using silver nanoparticles with three different morphologies. *Analytical Methods*, 8(37): 6691-6695, 2016.

[49] Chen, W., Cai, S., Ren, Q. Q., Wen, W., and Zhao, Y. D. Recent advances in electrochemical sensing for hydrogen peroxide: a review. *Analyst*, 137(1): 49-58, 2012.

[50] Semwal, V., and Gupta, B. D. Highly selective SPR based fiber optic sensor for the detection of hydrogen peroxide. *Sensors and Actuators B: Chemical*, 329: 129062, 2021.

[51] Singhal, G., Bhavesh, R., Kasariya, K., Sharma, A. R., and Singh, R. P. Biosynthesis of silver nanoparticles using *Ocimum sanctum* (Tulsi) leaf extract and screening its antimicrobial activity. *Journal of nanoparticle Research*, 13: 2981-2988, 2011.

[52] Rao, Y. S., Kotakadi, V. S., Prasad, T. N. V. K. V., Reddy, A. V., and Gopal, D. S. Green synthesis and spectral characterization of silver nanoparticles from Lakshmi tulasi (*Ocimum sanctum*) leaf extract. *Spectrochimica Acta Part A: Molecular and Biomolecular Spectroscopy*, 103: 156-159, 2013.

[53] Singh, J., Mehta, A., Rawat, M., and Basu, S. Green synthesis of silver nanoparticles using sun dried tulsi leaves and its catalytic application for 4-Nitrophenol reduction. *Journal of environmental chemical engineering*, 6(1): 1468-1474, 2018.

[54] Panda, S. K., Sen, S., Roy, S., and Moyez, A. Synthesis of colloidal silver nanoparticles by reducing aqueous $AgNO_3$ Using Green Reducing Agents. *Materials Today: Proceedings*, 5(3): 10054-10061, 2018.

[55] Kyrychenko, A., Pasko, D. A., and Kalugin, O. N. Poly (vinyl alcohol) as a water protecting agent for silver nanoparticles: The role of polymer size and structure. *Physical Chemistry Chemical Physics*, 19(13): 8742-8756, 2017.

[56] Kumar, D., Umrao, S., Mishra, H., Srivastava, R. R., Srivastava, M., Srivastava, A., and Srivastava, S. K. Eu: Y2O3 highly dispersed fluorescent PVA film as turn off luminescent probe for enzyme free detection of H_2O_2. *Sensors and Actuators B: Chemical*, 247: 170-178, 2017.

[57] Giguere, P. A., and Harvey, K. B. An infrared study of hydrogen bonding in solid H2O2 and H2O · H2O2 mixtures. *Journal of Molecular Spectroscopy*, 3(1-6): 36-45, 1959.

[58] Kumar, K. S., and Ramakrishnappa, T. Green synthesized uncapped Ag colloidal nanoparticles for selective colorimetric sensing of divalent Hg and H_2O_2. *Journal of Environmental Chemical Engineering*, 9(4): 105365, 2021.

[59] Jarujamrus, P., Amatatongchai, M., Thima, A., Khongrangdee, T., and Mongkontong, C. Selective colorimetric sensors based on the monitoring of an unmodified silver nanoparticles (AgNPs) reduction for a simple and rapid determination of mercury. *Spectrochimica Acta Part A: Molecular and Biomolecular Spectroscopy*, 142: 86-93, 2015.

[60] Borase, H. P., Patil, C. D., Salunkhe, R. B., Suryawanshi, R. K., Salunke, B. K., and Patil, S. V. Biofunctionalized silver nanoparticles as a novel colorimetric probe for melamine detection in raw milk. *Biotechnology and Applied Biochemistry*, 62(5): 652-662, 2015.

[61] Mauriz, E. Clinical applications of visual plasmonic colorimetric sensing. *Sensors*, 20(21): 6214, 2020.